## VI. Appendix

The derivation of Green's functions of this type is fairly well known and the details are not presented here. The following Green's functions relates an $x$ or $y$ directed magnetic current located on the $z = 0^-$ plane of Fig. 1 to the $H_x$ field on the same plane.

$$G_{xx}(x,x',y,y') = \sum_{n=1}^{\infty}\sum_{m=1}^{\infty} \frac{4}{abk_\rho^2}\left(\frac{k_x^2}{Z_E} + \frac{k_y^2}{Z_M}\right) \cdot \cos(k_y y)\ \cos(k_y y')\ \sin(k_x x)\ \sin(k_x x')$$

$$G_{xy}(x,x',y,y') = \sum_{n=1}^{\infty}\sum_{m=1}^{\infty} \frac{-4k_x k_y}{abk_\rho^2}\left(\frac{1}{Z_E} - \frac{1}{Z_M}\right) \cdot \sin(k_y y)\ \cos(k_y y')\ \cos(k_x x)\ \sin(k_x x') \quad \text{(A1)}$$

where

$$k_x = \frac{n\pi}{a}, \qquad k_y = \frac{m\pi}{b},$$
$$k_\rho^2 = k_x^2 + k_y^2, \qquad k_i = \sqrt{\varepsilon_{ri}k_0^2 - k_\rho^2}$$
$$Z_V = jZ_{TV1}\frac{Z_{TV2}\ \tan(k_2 d_2) + Z_{TV1}\ \tan(k_1 d_1)}{Z_{TV1} - Z_{TV2}\ \tan(k_2 d_2)\ \tan(k_1 d_1)} \quad \text{(A2)}$$

where

$$Z_{TMi} = \frac{k_i \eta_0}{\varepsilon_{ri}k_0}, \qquad Z_{TEi} = \frac{k_0\eta_0}{k_i},$$
$$V = E \ \text{ or } \ M, \qquad i = 1 \ \text{ or } \ 2.$$

## Acknowledgment

The author is grateful to M. M. Goldberg for very patiently fabricating and measuring the experimental circuits described in this paper.

## References

[1] R. Majidi *et al.*, "5-100 GHz InP CPW MMIC 7-section distributed amplifier," in *IEEE Monolithic Circuits Symp. Dig.*, May 1990, pp. 31–34.
[2] H. Shigesawa, M. Tsuji, and A. A. Oliner, "Conductor-backed slot-line and coplanar waveguide: Dangers and full wave analyses," in *IEEE MTT-S Microwave Symp. Dig.*, 1988, pp. 199–202.
[3] R. W. Jackson, "Mode conversion at discontinuities in modified grounded coplanar waveguides," in *IEEE MTT-S Int. Microwave Symp. Dig.*, 1988, pp. 203–206.
[4] ——, "Mode conversion at discontinuities in finite-width conductor-backed coplanar waveguide," *IEEE Trans. Microwave Theory Tech.*, vol. 37, pp. 1582–1588, Oct. 1989.
[5] M. Riaziat *et al.*, "Single mode operation of coplanar waveguides," *Electron. Lett.*, vol. 23, Nov. 19, 1987.
[6] R. W. Jackson, "Considerations in the use of coplanar waveguide for millimeter-wave integrated circuits," *IEEE Trans. Microwave Theory Tech.*, vol. MTT-34, pp. 1450–1455, Dec. 1986.
[7] J. J. Burke and R. W. Jackson, "A simple circuit model for resonant mode coupling in packaged MMICs," in *IEEE MTT Symp. Dig.*, Boston, MA, June 1990.
[8] E. Godshalk, "Wafer probing issues at millimeter wave frequencies," in *Proc. European Microwave Conf.*, 1992, pp. 925–930.

# CPW Oscillator Configuration for an Electro-Optic Modulator

Vesna Radišić, Vladan Jevremović, Zoya Basta Popović

***Abstract*— A CPW 2 GHz 3-port MESFET oscillator was designed with an electro-optic modulator application in mind. The oscillator has a self-biased gate. The source or drain ports can be used for external injection-locking. The frequency of oscillation, as well as the output power at the fundamental and first two harmonics were analyzed using a nonlinear device model and a harmonic balance technique. Comparison with measured results on a hybrid CPW oscillator fabricated on a Duroid substrate are presented.**

## I. Introduction

Recently, there has been great interest in gigabit modulation of guided optical signals for high data rate communications. A Mach–Zehnder modulator with electrodes in a push/pull configuration, fabricated with both $SiO_2$ and SiN buffer layers and indium tin oxide (ITO) was reported in [1]. The difficulty in the operation of wideband modulators is that the modulation is performed with an applied voltage. For a practical modulation index this voltage needs to be at least 5 V. The necessary modulating power decreases dramatically with the electrode structure. Izutsu *et al.* [2] presented a three-electrode coplanar waveguide modulator with a short circuited resonant line for the modulating electrode. Another analysis of CPW for $LiNbO_3$ optical modulators was presented in [3], but no active modulators for this purpose have been reported in the literature. The purpose of designing the CPW oscillator presented in this work is an efficient, compact, low power, active modulator with an open circuited resonant line for the modulating electrode. A 2-port superconductive CPW oscillator has been reported in the literature [4], but the approach taken here was to design a 3-port oscillator, and use the additional port for external injection-locking.

CPW is an attractive guiding medium for this application for a variety of reasons. Since the microwave voltage is applied between the central electrode and coplanar ground planes, many layers can potentially be stacked for dense electro-optic interconnects. The ground planes act as a good heat sink and monolithic implementation is compatible with active device layout, so that no via-holes are required. Further, although the widths of the gap and inner conductor are not fixed for a given impedance, their ratio is fixed. This allows for flexible design and high frequency operation.

## II. Design, Analysis and Measurement of the CPW Oscillator

The oscillator configuration is shown in Fig. 1. The analysis of the oscillator was done on Hewlett Packard's Microwave Design System (MDS) using transmission line circuit modeling. The device is a Fujitsu GaAs MESFET (FSC11FA/LG), which is a low noise device for C-band satellite communication receivers. The gate of the device is self-biased in order to minimize the number of bias points. The source and the drain are connected to 50Ω transmission lines. If needed, an additional bias line can be added at an appropriate place along the gate resonator. Since the gate is self-biased, and therefore the transistor is deep in saturation, a nonlinear analysis was performed.

Manuscript received September 20, 1992; revised February 1, 1992.
The authors are with the Department of Electrical and Computer Engineering, University of Colorado, Boulder, CO 80309-0425.
IEEE Log Number 9211843.

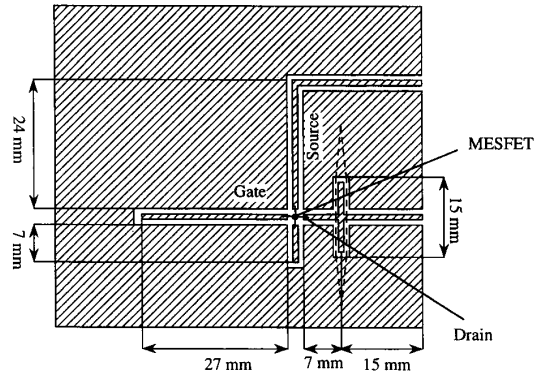


Fig. 1. The circuit layout. The gate of the MESFET is self-biased and is connected to a resonant section of open-circuited transmission line. The dashed line shows the possible position of optical waveguides in a Mach-Zehnder modulator. All CPW lines were designed to have impedances of 50Ω.

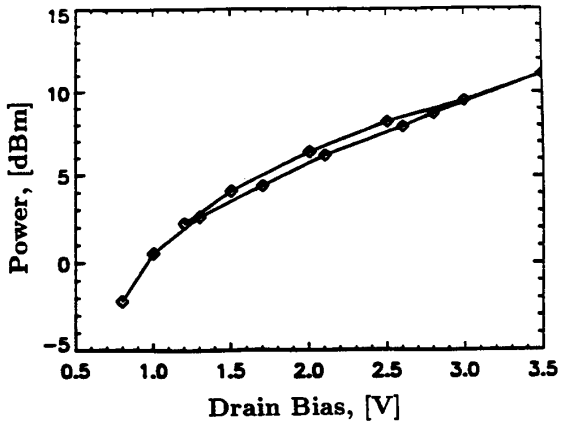


Fig. 2. Measured power of the fundamental frequency versus the drain voltage shows hysteresis, indicating a strong nonlinearity.

Quasi-static formulae for CPW [5] were used to design the CPW circuit:

$$Z_{0\mathrm{CPW}} = \frac{30\pi}{\sqrt{\frac{\epsilon_r+1}{2}}}\frac{K(k')}{K(k)} \tag{4}$$

where: $k = S/S + 2W, k' = \sqrt{1-k^2}, S$ is the width of the inner conductor, $W$ is the width of the gap, $\epsilon_r$ is relative dielectric constant of the substrate and $K(k)$ is the complete elliptic integral of the first kind. Equation (1) is valid for an infinite substrate thickness, but is still a good approximation for a substrate thickness greater than $3W$. From (1), for $\epsilon_r = 10.5$ and $Z_{0\mathrm{CPW}} = 50\Omega$, $k$ was calculated to be 0.5. This gives values of $S = 1.6$ mm and $W = 0.8$ mm, and since the substrate thickness is 2.54 mm, the $3W$ criterion is satisfied [5]. Another design consideration was the size of the ground plane. Equation (1) is valid for a ground plane that is greater then $5S = 8$ mm, which was taken into account in the final implementation. During the fabrication process of the circuit shown in Fig. 1, the widths of the gap and the inner conductor have changed. Their ratio remained the same, which would give the same characteristic impedance from (1). However, for the actual value of the gap width, the thickness of the substrate is no longer greater than $3W$, so equation (1) is not valid. Instead, experimental curves were used to find the characteristic impedance for a finite substrate thickness [5], which gave a $55\Omega$ impedance for all transmission lines.

In the experimental portion of this work, the source lead was connected to a $50\Omega$ load and the oscillation frequency and the power of the fundamental mode were measured using a HP 8593A spectrum analyzer as a function of the drain bias. The oscillation frequency of the fundamental mode $f_1$ was between 1.840 GHz and 1.905 GHz, depending on the drain voltage. The total change in frequency was 60 MHz, when $V_D$ was changed from 0.6 V to 3 V. Fig. 2 shows the measured power of the fundamental mode as a function of drain bias. There is a slight hysteresis in the power curve as the drain voltage is changed. All of the results correspond to values of power measured when the drain voltage is decreased. A Curtice cubic model was used for the transistor and a harmonic balance technique for circuit analysis [6]. The Curtice cubic model uses a third-order polynomial to describe the drain current. Fig. 3 shows the comparison between measured and predicted results for the frequency of oscillation of the fundamental mode as a function of the drain bias. The difference between measured and predicted values is at most 20 MHz for $V_D = 2.3$ V, a 1% difference. Fig. 4 shows the measured and modeled power for the first three harmonics. All three simulated

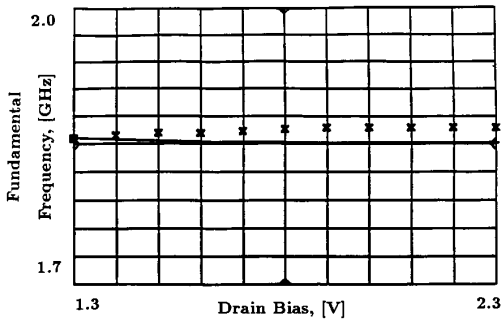


Fig. 3. The measured (cross symbols) and modeled (solid line) frequency of oscillation of the fundamental mode versus drain bias. The measured and theoretical values disagree by at most 20 MHz around 2 GHz (a 1% error).

curves follow the behavior of the measured ones. For the fundamental mode, the difference between the measured and predicted values is 1.5 dB for $V_D = 2.3$ V, while for the second harmonic it is between 3 dB (for $V_D = 2.3$ V) and 3.5 dB (for $V_D = 1.3$ V). For the self-biased oscillator, the gate voltage depends on the drain voltage; it drops as the drain voltage is decreased. However, in the MDS model the gate voltage is kept fixed as the drain voltage is swept, which might be the cause for discrepancies in the harmonic power levels. An experiment was also done with the drain terminated in a $50\Omega$ load and the oscillations in the source were measured. The frequency of oscillation remained almost unchanged, but the power was different. Table I shows the power of the fundamental mode in the source and in the drain versus the drain bias $V_D$. As $V_D$ goes up, the drain port proportionally takes up more of the power.

An external injection-locking signal can be injected in the source for modulation purposes or for reducing the oscillator noise. The injection-locking bandwidth of the oscillator was measured versus the injected power. The locking bandwidth depends on the applied drain voltage with results shown in Fig. 5 on a logarithmic scale. Many authors have shown experimentally that the locking range is proportional to the square root of the injected power [7]–[9], as long as the injected power is kept sufficiently low. This relationship occurs here, as well. However, as the injected power increases above −14dBm, the injection locking range power dependance deviates from the square root relationship. This can be seen in Fig. 5, where the dashed line shows a slope of $1/2$, corresponding to the square root

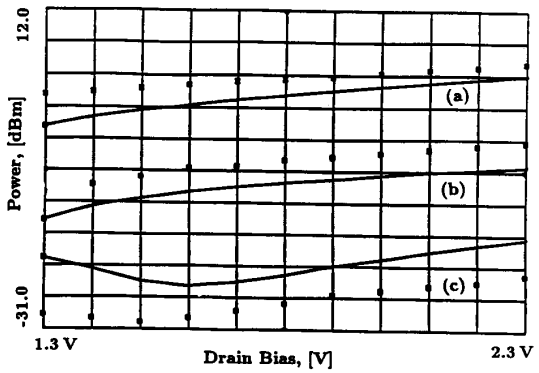


Fig. 4. Power of the fundamental (a), second (b) and third harmonic (c) versus the drain bias voltage. The nonlinear simulation is shown in solid line and the measured results with cross symbols.

TABLE I
POWER OF THE FUNDAMENTAL MODE IN THE SOURCE AND IN THE DRAIN VERSUS DRAIN BIAS

| $V_D$ | power-source | power-drain | difference |
|---|---|---|---|
| [V] | [dBm] | [dBm] | [dB] |
| 1.0 | −4.8 | 0.6 | 5.4 |
| 1.5 | −3.0 | 3.4 | 6.4 |
| 2.0 | −1.6 | 5.5 | 7.1 |
| 2.5 | −0.9 | 6.5 | 7.4 |
| 3.0 | 0.1 | 7.7 | 7.6 |
| 3.5 | 1.5 | 9.3 | 7.8 |
| 3.7 | 2.2 | 10.2 | 8.0 |

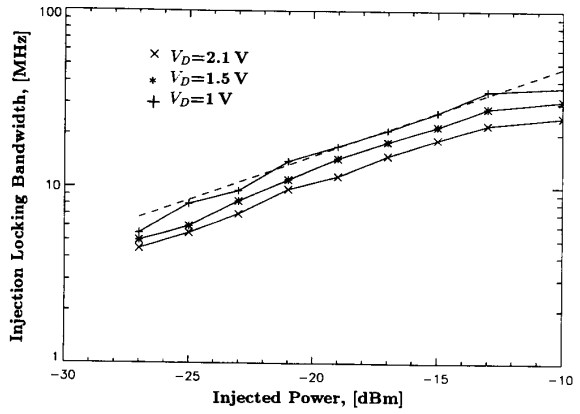


Fig. 5. Measured injection-locking bandwidth versus power injected into the source shows a square root dependance with injected power for small injected power levels. The dashed line has a slope of 1/2, for comparison.

of the injected power. The loaded Q-factor is found from injection-locking measurements [9] to be between 10 and 13, depending on the bias point.

## III. CONCLUSION

A three-port MESFET oscillator built in CPW technology was demonstrated at 1.9 GHz for $V_D = 3$ V with an output power of 8 dBm. Such an oscillator topology on a GaAs or any other electro-optic substrate should be suitable for high-speed electro-optic modulator applications. For an efficient optical modulator, one needs a voltage around 5 V across the optical waveguides, shown in dashed line in Fig. 1. In the oscillator presented in this paper, this voltage was around 1 V. A possibility for improvement is to use a higher power transistor, and to optimize the circuit structure for higher impedance, thereby reducing the current. This could be done by increasing the output load, which changes the operating point of the device (load pulling). The resulting relative voltage increase is larger than the relative power increase, which is advantageous for minimizing output power while maximizing the output voltage used to modulate the optical signal. This is also an advantage for devices built on temperature sensitive organic materials, such as nonlinear optical polymers [10].

## ACKNOWLEDGMENT

We thank Hewlett Packard for their generous equipment donation that made this work possible, and Rogers and Fujitsu for their substrate and device donations.

## REFERENCES

[1] W. Charczenko, M. Surette, R. Fox, S. Vohra, A. Mickelson and S. Asher, "Comparison of numerical simulations to experimental measurements of proton exchanged and annealed channel waveguides and directional couplers in $LiNbO_3$," *Integrated Photonics Research Conf.*, Monterey, CA, Apr. 1991.

[2] M. Isutsu, "Millimeter wave light modulator using $LiNbO_3$ waveguide with resonant electrode," *Proc. CLEO Conf.*, paper PD14, Anaheim, CA, Apr. 1988.

[3] T. Kitazawa, D. Polifko, and H. Ogawa, "Analysis of CPW for $LiNbO_3$ optical modulator by extended spectral-domain approach," *IEEE Microwave Guided Wave Lett.*, vol. 2, no. 8, pp. 313–315, Aug. 1992.

[4] R. Klieber, R. Ramish, A. A. Valenzuela, R. Weigel and P. Russer, "A coplanar transmission line high-$T_C$ superconductive oscillator at 6.5 GHz on a single substrate," *IEEE Microwave Guided Wave Lett.*, vol. 2, no. 1, pp. 22–24, Jan. 1992.

[5] K. C. Gupta, Ramesh Garg, and I. J. Rahe, *Microstrip Lines and Slotlines*, Norwood, MA: Artech House, 1979, pp. 257–267.

[6] *HP 85150B Microwave Design System Component Catalog*, vol. 2, Software Revision B.03.00, Hewlett Packard, Feb. 1991.

[7] B. W. Hakki and J. P. Beccone, "Phase-locked GaAs microwave oscillators," *IEEE Trans. Electron Devices*, vol. ED-13, pp. 197–199, Jan. 1966.

[8] R. C. Show and H. L. Stover, "Phase-locked avalanche diode oscillators," *Proc. IEEE (Lett.)*, vol. 54, pp. 710–711, Apr. 1966.

[9] K. Kurokawa, "Injection-locking of microwave solid-state oscillators," *Proc. IEEE*, vol. 61, pp. 1386–1410, Oct. 1973.

[10] M. Stahelin, D. M. Burland, M. Ebert, R. D. Miller, B. A. Smith, R. J. Twieg, W. Volksen, and C. A. Walsh, "Reevaluation of the thermal stability of optically nonlinear polymeric quest-host systems," *Appl. Phys. Lett.*, vol. 61, pp. 1626, 1992.